2019 American Control Conference (ACC)
Philadelphia, PA, USA, July 10-12, 2019

Geometric Control of a Quadrotor with a Load Suspended from an Offset

Jun Zeng and Koushil Sreenath

***Abstract*— A quadrotor with a point-mass payload suspended with an offset from the center-of-mass of the quadrotor to the suspension point is studied in this paper. This system consists of eight degrees of freedom and four degrees of underactuation. A coordinate-free dynamic model is obtained by taking variations on manifolds. We also establish that under a mild assumption that the angular acceleration of quadrotor is small, the offset quadrotor-load system is a differentially-flat system with the load position and the quadrotor yaw serving as the flat outputs. A nonlinear geometric control design based on this assumption is developed. With this controller, the following states (a) quadrotor attitude, (b) load attitude, and (c) load position can be tracked. Stability proofs for the controller design, as well as simulation of the proposed controller are presented. A comparison of a geometric controller developed for a zero offset quadrotor-load model is also presented to motivate the need as well as demonstrate the advantages of our proposed geometric controller for the offset quadrotor-load model.**

I. Introduction

Unmanned aerial vehicles (UAVs), such as quadrotors, have led to a variety of applications in society. In the area of manipulation, quadrotors have been used for transportation of external loads. There are various approaches in realizing aerial manipulation and transportation. One of them is using aerial robots equipped with fixed grippers, where the payload is rigidly attached to the aerial robot through the gripper, and the same control technique for flying without a load is used. These robots are typically characterized by slow, quasi-static motions for hovering and picking up objects, see [5]. One exception to this is the work on avian-inspired aerial pickup in [12]. However, carrying an external load through a gripper increases the inertia of the system considerably and results in the quadrotor exhibiting a sluggish attitude response, therefore making it less robust to perturbations. An alternative method is to suspend loads through a cable, in order to retain the agility of the aerial vehicle while achieving the task of transportation of the suspended load. Here the quadrotors can range in size from centimeters to meters with payloads up to several kilograms.

We know that cable-suspended systems are underactuated, and several control approaches have been studied in recent years. Early research in this area has focused on minimizing the load swing through a combination of trajectory generation and active feedback control, see [7], [10]. The idea is to model the cable as a massless rigid rod when it is taut and also model the transitions between the cable going from taut to slack and slack to taut. Hybrid system modelling and differential flatness have been applied to generate desired trajectories. Earlier work in [6] applied a dynamic programming approach to generate dynamically feasible trajectories. Based on the massless rigid rod model, prior work in [8], [9] derived a coordinate-free dynamical model of a single quadrotor with suspended load and developed a geometric controller to exponentially track the load position. These results have been utilized to plan trajectories to avoid collision with obstacles, see [11]. The problem of geometric control of multiple quadrotors with a suspended point-mass load [4] or with a rigid-body load [3], [13] are also studied. Recently, the dynamics and control of a quadrotor with a point-mass payload suspended through several flexible cables was also studied [2].

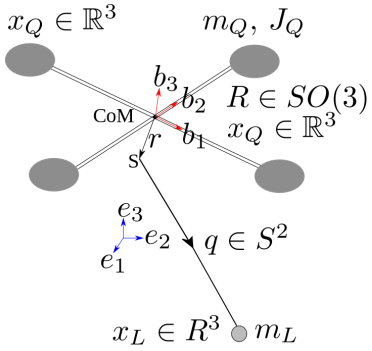

Fig. 1. A quadrotor with a cable suspended load, where the offset vector exists from the CoM of the quadrotor to the suspension point S. When the cable is taut, the system evolves on $\mathbb{R}^3 \times S^2 \times SO(3)$, and has 8 degrees of freedom with 4 degrees of underactuation. The vector r represents the offset from the CoM of quadrotor to the suspension point S.

A critical assumption in all prior work is that the cable is suspended from the quadrotor's center-of-mass (CoM), and no offset vector exists from the CoM of the quadrotor to the suspension point. In the real world, it's hard to figure out where the CoM lies exactly. Even if the position of the CoM is precisely known, maybe it is impossible for us to attach a cable at that position. For instance, the CoM could lie inside the body or battery components. If an offset from the suspension point to the CoM exists, the cable not only exerts additional moment on the quadrotor, resulting in the quadrotor attitude dynamics being coupled to load dynamics, but also breaks the differential-flatness property, which is a key method used in prior work to generate dynamically-feasible trajectories [8]. An illustration of a quadrotor with a load suspended with an offset is presented in Figure 1. In this paper, we take the offset vector from the CoM of quadrotor to the suspension point into consideration and the goal is to investigate the design of controllers for this dynamical

Jun Zeng and Koushil Sreenath are with Department of Mechanical Engineering, UC Berkeley, Hearst Ave 6141, Berkeley, CA 94720, {zengjunsjtu, koushils}@berkeley.edu.

This work is supported in part by NSF grant CMMI-1840219.

TABLE I

VARIOUS SYMBOLS USED IN THE PAPER

$\mathscr{B}$, $\mathscr{W}$	Body-fixed and world frame
$m_Q \in \mathbb{R}$	Mass of quadrotor
$m_L \in \mathbb{R}$	Mass of suspended load
$J_Q \in \mathbb{R}^{3\times3}$	Inertia matrix of the quadrotor in $\mathscr{B}$
$R \in SO(3)$	Rotation matrix from the body-fixed frame to inertial frame
$\Omega \in \mathbb{R}^3$	Angular velocity of the quadrotor in $\mathscr{B}$
$\omega \in \mathbb{R}^3$	Angular velocity of the suspended load in $\mathscr{W}$
$x_L, v_L \in \mathbb{R}^3$	Position and velocity vectors of load in $\mathscr{W}$
$f \in \mathbb{R}$	Magnitude of the thrust for the quadrotor
$M \in \mathbb{R}^3$	Moment vector for the quadrotor in $\mathscr{B}$
$q \in S^2$	Unit vector from the suspension point to the load in $\mathscr{W}$
$L \in \mathbb{R}$	Length of cable
$e_1, e_2, e_3 \in \mathbb{R}^3$	Unit vectors along the x, y, z directions of $\mathscr{W}$
$b_1, b_2, b_3 \in \mathbb{R}^3$	Unit vectors along the x, y, z directions of $\mathscr{B}$ in $\mathscr{W}$
$r \in \mathbb{R}^3$	Offset vector from the quadrotor's CoM to the suspension point on the quadrotor in $\mathscr{B}$

model. The contributions of this paper with respect to prior work are:

- We consider the quadrotor with a cable-suspended load, where there exists an offset from the center-of-mass of the quadrotor to the load suspension point. For the rest of paper, we refer to this dynamical model as the "offset dynamical model". We derive the dynamics in a coordinate-free manner using Lagrange-d'Alembert principle.
- Based on the assumption of low angular acceleration of quadrotor, the differential flatness property is established for the offset dynamical model and the necessity of this assumption to build the control design is explained.
- Under the assumption of low angular acceleration of the quadrotor, we develop a geometric control design for the offset dynamical model based on the prior work [8], and we provide a stability analysis using singular perturbations.
- We present numerical results of tracking the load position and compare the offset geometric control design performance with the prior one to quantitatively evaluate the advantages.

The paper is organized as follows. Section II develops a coordinate-free model for the offset dynamical system. Section III demonstrates that the flat outputs in the zero offset dynamical system cannot be used as the flat outputs in the offset dynamical model. To handle this problem, we assume the angular acceleration of the quadrotor to be small, so that the differential flatness property for geometric control design can be retained. Section IV presents the main result of our geometric control design for the offset dynamical model. Section V shows the simulation results of the offset dynamical model for tracking desired trajectories. In addition, a comparison about the convergence performance of load position error with the prior work in [8] is studied.

II. DYNAMIC MODEL WITH NONZERO CABLE TENSION

A. Dynamical Model with Nonzero Cable Tension

The configuration of the system is defined by the location of the load with respect to the inertial frame, the load attitude and the quadrotor attitude. When the cable is taut, the system has eight degrees-of-freedom with configuration space $Q = \mathbb{R}^3 \times S^2 \times SO(3)$ and four degrees-of-underactuation. The quadrotor and load positions x_Q and x_L are related by

$$x_Q = x_L - Lq - Rr \tag{1}$$

where r is the offset vector from the quadrotor's CoM to the suspension point on the quadrotor in the body-fixed frame, q represents the unit vector from the suspension point to the load and L is the length of cable. Other symbols used in the paper are defined in Table I.

The method of Lagrange-d'Alembert principle is used to develop the dynamical equations of motion. The Lagrangian for the system is defined by $\mathscr{L} = \mathscr{T} - \mathscr{U}$, where $\mathscr{T}$ and $\mathscr{U}$ are kinetic and potential energies of the mechanism, respectively, and defined as,

$$\mathscr{T} = \frac{1}{2}m_Q||v_Q||^2 + \frac{1}{2}\Omega^T J\Omega + \frac{1}{2}m_L||v_L||^2, \tag{2}$$

$$\mathscr{U} = m_Q g e_3 \cdot x_Q + m_L g e_3 \cdot x_L. \tag{3}$$

As a result of the dynamics of the system satisfying the Lagrange-d'Alembert principle, we have

$$\delta \int_{t_0}^{t_1} \mathscr{L} dt + \int_{t_0}^{t_1} (\langle W_1, \hat{M}\rangle + W_2 \cdot f R e_3) dt = 0, \tag{4}$$

where f is the thrust magnitude, M is the moment vector, and $W_1 = R^T\delta R$, $W_2 = \delta x_Q = \delta x_L + \delta R r - L\delta q$ are variational fields with the infinitesimal variations satisfying,

$$\delta R = R\hat{\eta}, \delta\Omega = \Omega\eta + \dot{\eta}, \eta \in \mathbb{R}^3, \tag{5}$$

$$\delta q = \xi \times q, \delta\dot{q} = \dot{\xi} \times q + \xi \times \dot{q}, \xi \in \mathbb{R}^3 \text{ s.t. } \xi \cdot q = 0, \tag{6}$$

where δq is a variation on S^2, and δR a variation on $SO(3)$.

The equations of motion can be obtained from the above equations and the fact that (4) is satisfied for all variations δq and δR. The detailed computation can be found in Appendix A, resulting in,

$$A\begin{bmatrix}\ddot{x}_L + ge_3 \\ \dot{\Omega}\end{bmatrix} = \begin{bmatrix}G_1 \\ G_2\end{bmatrix}u^{\parallel} + \begin{bmatrix}d_1 \\ d_2\end{bmatrix} + \begin{bmatrix}0 \\ M - \Omega \times J_Q\Omega\end{bmatrix}, \tag{7}$$

$$\dot{R} = R\hat{\Omega}, \tag{8}$$

$$\dot{q} = \omega \times q, \tag{9}$$

$$\dot{\omega} = -\hat{q}u^{\perp} + q \times \frac{1}{L}(\ddot{x}_L + ge_3 - R(\hat{\Omega}^2 + \dot{\hat{\Omega}})r), \tag{10}$$

where (7)-(8) describes the coupled dynamics for load position and quadrotor attitude and (9)-(10) describes the coupled dynamics between the load position and load attitude. In these equations of motion, $u^{\parallel} = (u \cdot q) \cdot q$ and $u^{\perp} = -\hat{q}^2 u$ represent the parallel and perpendicular vectorial projection of u on q, where $u = \dfrac{f}{m_Q L} R e_3$. The equivalent mass matrix

and inertial tensor are described in matrix A, where

$$A = \begin{bmatrix} A_{11} & A_{12} \\ A_{21} & A_{22} \end{bmatrix} = \begin{bmatrix} m_L I_3 + m_Q q q^T & m_Q q q_b^T \hat{r} \\ -m_Q \hat{r} q_b q^T & J_Q + m_Q (\hat{r} q_b)(\hat{r} q_b)^T \end{bmatrix}, \tag{11}$$

where $q_b = R^T q$ represents directional vector of the cable in the body-fixed frame. Other terms in the equations of motion are presented below,

$$G_1 = m_Q L q q^T, \quad G_2 = -m_Q L \hat{r} q_b q^T,$$
$$d_1 = m_Q (q_b^T \hat{\Omega}^2 r - L(\omega \cdot \omega)) q,$$
$$d_2 = -m_Q (q_b^T \hat{\Omega}^2 r - L(\omega \cdot \omega))(\hat{r} q_b).$$

We will refer to the above model as the *offset model*. If the offset vector r is zero, the equations of motion turn out to be the same as [8, Equations (5)-(10)], whose geometric control design was fully studied in that paper. In the following sections, we refer to the model with r equal to zero as the *zero offset model*.

Remark 1: From (7), we notice that the load position and quadrotor attitude dynamics are coupled and controlled by $u^{\parallel}$ and M, and their dynamics are decoupled when the offset vector becomes zero. This means the tension in the cable will influence both the translational and the rotational dynamics of the quadrotor. Moreover, we notice that the evolution of the load attitude depends on the angular acceleration of the quadrotor's attitude $\dot{\Omega}$ from (10).

B. Dynamical Model with Zero Cable Tension

When the tension in the cable becomes zero, the quadrotor will be decoupled from the load, and the load will be in free fall. The dynamical model in this case is,

$$\dot{x}_L = v_L, \quad m_L(\dot{v}_L + g e_3) = 0, \tag{12}$$
$$\dot{x}_Q = v_Q, \quad m_Q(\dot{v}_Q + g e_3) = f R e_3, \tag{13}$$
$$\dot{R} = R\hat{\Omega}, \quad J_Q \dot{\Omega} = M - \Omega \times J_Q \Omega. \tag{14}$$

Remark 2: The quadrotor with a cable suspended load is a hybrid system since the dynamics switch when the tension in the cable becomes zero, or when the slack cable becomes taut which implies the tension is reestablished.

III. Differential Flatness

A system is differentially-flat, if there exists a set of outputs such that the system states and the inputs can be expressed in terms of the flat output and a finite number of its derivatives. We explain the differential flatness of the offset dynamical system by introducing several lemmas.

Remark 3: The flat output $Y_1 = (x_L, \psi)$, which was proved to be the set of flat outputs for the zero offset system in [9], cannot be regarded as the flat outputs for the offset quadrotor-load system. Here $\psi \in \mathbb{R}$ is the yaw angle of the quadrotor.

This can be seen as follows: from $x_L(t)$, we can compute the cable tension $T := m_L(g e_3 + \dot{v}_L)$ and the load attitude $q = -\frac{T}{||T||}$. The quadrotor position can be determined by $x_Q(t) = x_L(t) - Lq(t) - R(t)r$. From [9], we know $R(t)$ is a function of $\ddot{x}_Q(t)$ and $\psi(t)$. We thus note $R = h(\ddot{x}_Q, \psi)$. Therefore, the geometric relation between x_Q and the flat outputs becomes:

$$x_Q(t) = x_L(t) - Lq(t) - h(\ddot{x}_Q(t), \psi(t))r, \tag{15}$$

which indicates x_Q cannot be solved unless we have additional information about $\ddot{x}_Q$. Hence the system is not differentially flat with the flat output Y_1.

Lemma 1: When the angular acceleration of quadrotor is small, we can reestablish the differential flatness property with flat output $Y_1 = (x_L, \psi)$.

Proof: For a small time interval Δt, we can approximate (15) as

$$x_Q(t + \Delta t) = x_L(t + \Delta t) - Lq(t + \Delta t) - R(t)r. \tag{16}$$

Moreover, under the assumption of low angular acceleration of quadrotor, we also have,

$$\dot{R} = R\hat{\Omega}, \quad \ddot{R} = R\hat{\Omega}^2 + R\dot{\hat{\Omega}} \approx R\hat{\Omega}^2.$$

Similarly for other high order derivatives of R, we have

$$\frac{d^n R}{dt^n} = R\hat{\Omega}^{n-1}. \tag{17}$$

Thus for $n \in [1,4]$,

$$\frac{d^n x_Q}{dt^n}(t + \Delta t) = \frac{d^n x_L}{dt^n}(t + \Delta t) - L\frac{d^n q}{dt^n}(t + \Delta t) - R(t)\hat{\Omega}(t)^{n-1} r. \tag{18}$$

According to [9], these high order derivatives of x_Q are sufficient to calculate all other states and inputs to reestablish differential flatness. Note that $R(t + \Delta t)$ is computed from $x_Q(t + \Delta t)$ and its higher order derivatives. ■

IV. Control Design

Having computed the dynamics of the system containing a quadrotor with a cable suspended load attached with an offset from the CoM, and shown that under the low angular acceleration assumption, the load position and yaw angle forms a set of differentially-flat outputs. we will now develop a controller that can be used for tracking one of the following quantities (a) quadrotor attitude, (b) load attitude, or (c) load position.

A. Configuration Errors

Before proceeding to describe the different controllers, we firstly define the configuration error for different variables. Given a smooth attitude tracking command $R_d(t) \in SO(3)$, the angular velocity related to the attitude tracking command can be obtained by the kinematics equation, $\dot{\Omega}_d = R_d^T \dot{R}_d$. The real-valued error function on the manifolds $SO(3) \times SO(3)$ is then defined as

$$\Psi_R = \frac{1}{2} Tr(I - R_d^T R). \tag{19}$$

The configuration error Ψ_R for the manifold $SO(3) \times SO(3)$ has a maximum value of 2, when the actual rotation matrix and desired one have the opposite direction and becomes zero when $R = R_d$. Based on this notation, the vector error functions of e_R and e_Ω on $TSO(3)$ are given by

$$e_R = \frac{1}{2}(R_d^T R - R^T R_d)^\vee, \quad e_\Omega = \Omega - R^T R_d \Omega_d, \tag{20}$$

where R_d and Ω_d are the desired rotation matrix and angular velocity of the quadrotor.

Similarly, the configuration error for the S^2 manifold is given as $\Psi_q = 1 - q_d^T q$, where q_d^T is the desired load-attitude,

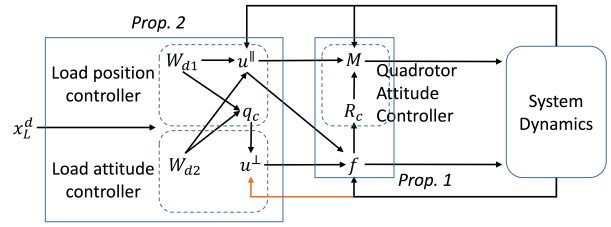

Fig. 2. Block diagram of the controller structure. The dashed blocks illustrate load position, load attitude and quadrotor attitude controllers, respectively. The inner-outer feedback is presented and two propositions of stability and convergence (see their proofs at the end of Section IV) are circled. The orange arrow indicates that the controller is established based on low angular acceleration of quadrotor, where we ignore a term of $\dot{\Omega}$ for the control design of (26).

and error functions for q and $\dot{q}$ are given as follows,

$$e_q = \hat{q}^2 q_d, \quad e_{\dot{q}} = \dot{q} - (q_d \times \dot{q}_d) \times q. \tag{21}$$

Error functions for position and velocity of the load are

$$e_x = x_L - x_L^d, \quad e_v = v_L - v_L^d, \tag{22}$$

where x_L^d and v_L^d are the desired position and velocity of the load.

B. Control Algorithm

The geometric controller for the zero offset dynamical model has been well studied [8]. However, if we apply this controller to the offset dynamical model, there will be a large error in tracking the load position, which we illustrate by a numerical simulation in Section V. Therefore, we need to propose a control design for the offset dynamical model. The goal of our geometric controller is to track one of the following variables (a) quadrotor attitude (b) load attitude or (c) load position. Figure 2 illustrates the inner-outer loop controller structure for the load position tracking.

For the later discussion, we call the geometric controller for the zero offset model described in [8] as $\mathscr{C}_Z$ and we call our geometric controller for the offset model described in Section IV as $\mathscr{C}_O$.

The control design operates as shown below,

Step 1: From dynamics in (7), we can compute a feed forward and PD feedback wrench $W_d = \begin{bmatrix} W_{d1} \\ W_{d2} \end{bmatrix}$, defined as

$$W_d = \begin{bmatrix} \ddot{x}_L^d + ge_3 - k_x e_x - k_v e_v \\ -\hat{\Omega} R^T R_d \Omega_d + R^T R_d \dot{\Omega}_d - \dfrac{k_R}{\varepsilon^2} e_R - \dfrac{k_\Omega}{\varepsilon} e_\Omega \end{bmatrix}, \tag{23}$$

where e_R, e_Ω, e_x, e_v are defined in (20) and (22). Note that $\dot{\Omega}_d, R_d$ can be calculated from the differential flatness based on the assumption of low angular acceleration of quadrotor as presented in Lemma. 2.

Step 2: Use the desired wrench to calculate the parallel component of u,

$$u^{\parallel} = [(A_{11}W_{d1} + A_{12}W_{d2} - d_1)/||G_1||_2 \cdot q] \cdot q, \tag{24}$$

and also the desired load attitude

$$q_c = -\frac{A_{11}W_{d1} + A_{12}W_{d2} - d_1}{||A_{11}W_{d1} + A_{12}W_{d2} - d_1||}. \tag{25}$$

Remark 4: The choice of the control for $u^{\parallel}$ follows from the dynamics in (7), resulting in $G_1 u^{\parallel} = [(A_{11}W_{d1} + A_{12}W_{d2} - d_1) \cdot q] \cdot q$ since $||G_1||_2 = m_Q L$ and it's not invertible. This control design was motivated from work in [13] for multiple quadrotors, however they employ the Moore-Penrose inverse of matrix $G = \begin{bmatrix} G_1 \\ G_2 \end{bmatrix}$.

Step 3: Based on this, we are able to cancel out the effects of load acceleration on the cable attitude using the perpendicular part of u as follows. From the load attitude dynamics in (10) and since q is parallel to $\ddot{x}_L + ge_3$, we can define a geometric controller for $u^{\perp}$ as,

$$\begin{aligned} u^{\perp} &= -k_q e_q - k_\omega e_{\dot{q}} - \langle q, q_d \times \dot{q}_d \rangle (q \times \dot{q}) \\ &\quad - (q_d \times \ddot{q}_d) \times q + \frac{1}{L}\hat{q}^2 R(\hat{\Omega}^2 + \dot{\hat{\Omega}}) r \\ &\approx -k_q e_q - k_\omega e_{\dot{q}} - \langle q, q_d \times \dot{q}_d \rangle (q \times \dot{q}) \\ &\quad - (q_d \times \ddot{q}_d) \times q + \frac{1}{L}\hat{q}^2 R \hat{\Omega}^2 r. \end{aligned} \tag{26}$$

Here we have ignored the last term $\frac{1}{L}\hat{q}^2 R\dot{\hat{\Omega}} r$, based on the assumption of low angular acceleration of the quadrotor. The configuration error of q is defined in (21) and we use the calculated load attitude in (25) to represent the desired load attitude q_d in (26). The above approximation is highlighted in orange in Figure 2.

Step 4: Next, define $v = m_Q L(u^{\parallel} + u^{\perp})$, where $u^{\parallel}$ and $u^{\perp}$ are defined in (24), (26). The thrust of quadrotor is defined as

$$f = v \cdot Re_3 = m_Q L(u^{\parallel} + u^{\perp}) \cdot Re_3, \tag{27}$$

and the computed quadrotor attitude is defined as

$$R_c := [b_{1c}; b_{3c} \times b_{1c}; b_{3c}], \quad \hat{\Omega}_c = R_c^T \dot{R}_c, \tag{28}$$

where $b_{3c} \in S^2$ is defined by

$$b_{3c} = \frac{m_Q L(u^{\parallel} + u^{\perp})}{||m_Q L(u^{\parallel} + u^{\perp})||}, \tag{29}$$

and we choose desired yaw orientation $b_{1d} \in S^2$ not parallel to b_{3c} and define

$$b_{1c} = -\frac{1}{||b_{3c} \times b_{1d}||}(b_{3c} \times (b_{3c} \times b_{1d})). \tag{30}$$

As computed orientation R_c and Ω_c are known, we recalculate W_{d2} by using R_c, Ω_c instead of the desired ones R_d, Ω_d from the differential flatness based on the assumption of low angular acceleration of quadrotor.

Step 5: Finally, from the dynamics in (7), we can compute the moment of the quadrotor with a geometric controller as follows

$$M = \Omega \times J_Q \Omega + A_{21}W_{d1} + A_{22}W_{d2} - G_2 u^{\parallel} - d_2. \tag{31}$$

Remark 5: In the control design, approximations based on the assumption of low angular acceleration of quadrotor are used in Steps 1 and 3. In Step 1, we generate desired states $\dot{\Omega}_d$ and R_d based on the assumption of low angular acceleration of the quadrotor and the approximate geometric relation in (16). If $R_d, \Omega_d, \dot{\Omega}_d$ were available through a dynamically feasible planner, then this assumption is not required in Step 1. In Step 3, the canceling term of $\frac{1}{L}\hat{q}^2 R\dot{\hat{\Omega}} r$ is ignored due to the same assumption of low angular acceleration of the quadrotor.

Proposition 1: (Almost Global Exponential Tracking of Force and Yaw based on the assumption of low angular accel-

eration of Quadrotor) Consider a desired force v to be applied by a quadrotor with a desired quadrotor yaw orientation b_{1d}, defined in Step 4. Also consider the following quadrotor inputs f, M, defined in (27), (31), respectively. Then there exists parameters k_R, k_Ω and $\bar{\varepsilon}$ such that the errors $v - fRe_3$ and $R - R_d$ tend to be almost exponentially convergent when $\varepsilon < \bar{\varepsilon}$. Moreover, the convergence rate can be increased by reducing the value of ε.

Proof: By substituting (31) into (7), we have

$$\varepsilon \begin{bmatrix} e_R \\ \dot{e}_\Omega \end{bmatrix} = \begin{bmatrix} \frac{1}{2}(tr(R^T R_c) I_3 - R^T R_c) e_\Omega \\ -k_R \frac{e_R}{\varepsilon} - k_\Omega e_\Omega \end{bmatrix}. \tag{32}$$

By [8, Prop. 1], there exist suitable positive values for k_R, k_Ω and $\bar{\varepsilon}$ such that the R could track R_d exponentially. In addition, ε plays a role in controlling the convergence rate.

On the other hand, the error between actual and desired thrust vector of the quadrotor is

$$fRe_3 - v = (b_{3c} - (b_3 \cdot b_{3c}) b_3) \cdot ||v||. \tag{33}$$

Since the attitude tracking is exponentially convergent, b_{3c} will converge to b_3, in addition to the boundedness of v, we have the thrust vector convergent to v exponentially. ∎

Proposition 2: (Almost Global Input-to-State Stability of Tracking the Load Position and Load Attitude based on the assumption of low angular acceleration of Quadrotor) Consider reduced system for load position and attitude, defined in (7), (9), (10). Also consider the desired force to be applied by the quadrotor as,

$$v = m_Q L (u^{\parallel} + u^{\perp}), \tag{34}$$

where $u^{\parallel}$ and $u^{\perp}$ are defined in (24) and (26). Then there exists gain parameters k_x, k_v, k_q, $k_{\dot{q}}$ such that the reduced system tracks the reference output q_d, x_L^d. When the angular acceleration of quadrotor is low, this tracking is almost globally exponentially stable, otherwise we obtain almost global input-to-state stability.

Proof: When the angular acceleration of the quadrotor is low, by substituting (24), (26) into (7), (10), we have

$$\ddot{e}_x = -k_x e_x - k_v e_v, \tag{35}$$

$$\ddot{e}_q = -k_q e_q - k_{\dot{q}} e_{\dot{q}}, \tag{36}$$

where load position and cable attitude errors are totally decoupled from each other. Thus we could treat each of them as independent subsystems. As well-studied in [13], [3], there exist suitable gains k_x, k_v, k_q, $k_{\dot{q}}$ to ensure the exponential convergence.

Since we calculate W_{d2} by explicit differential flatness based on the assumption of low angular acceleration of the quadrotor and the approximate geometric relation in (16), when this assumption fails, we obtain an error X, representing the difference between the approximately calculated W_{d2} in (23) and the exact one,

$$X = W_{d2} - W_{d2}^{exact}. \tag{37}$$

W_{d2}^{exact} is the exact value of W_{d2}, where we don't assume the approximate geometric relation in (16) and the low angular acceleration of quadrotor. In that case, expressions of R_d, Ω_d, $\dot{\Omega}_d$ need to be computed by solving the differential equation in (15) and we don't know their explicit expressions. Hence we cannot present the explicit expression of W_{d2}^{exact}.

We also define

$$Y = \frac{1}{L} \hat{q}^2 R \hat{\dot{\Omega}} r, \tag{38}$$

representing the ignored canceling term in (26). By taking the two approximation errors into account, the error dynamics of load position and attitude can be written as,

$$\ddot{e}_x = -k_x e_x - k_v e_v + P(X), \tag{39}$$

$$\dot{e}_\omega = -k_q e_q - k_\omega e_\omega + Q(Y), \tag{40}$$

where $P(X)$, $Q(Y)$ are two bounded nonlinear functions, representing the errors from approximation which influences the error dynamics of load position and attitude. If the angular acceleration of the quadrotor is small, we can assume $X = Y = 0$, where we have the exponential convergence. If $\dot{\Omega}$ is not small, our controller only has the input-to-state stability. In this case, we will observe a bounded final error of load position e_x and load attitude e_q. ∎

Remark 6: Since we only have the input-to-state stability of tracking load position and load attitude instead of exponential stability, a small final error of load position tracking occurs when the acceleration of the quadrotor is not small. The peak payload position error depends on how aggressively the quadrotor moves, which we quantify later in Figure 5.

Proposition 3: (Almost Global Input-to-State Stability of Tracking the Full System based on the assumption of low angular acceleration of Quadrotor) Consider the full model of the system which includes the quadrotor dynamics, with virtual control v specified in Prop. 1 and f, M specified in Prop. 2, Then there exists parameters $k_x, k_v, k_q, k_{\dot{q}}, k_R, k_\Omega$ and $\bar{\varepsilon}$, such that when $\varepsilon < \bar{\varepsilon}$, the reference outputs (x_L^d, q_d, R_d) are tracked for the closed-loop full system, based on the assumption of low angular acceleration of the quadrotor. If the angular acceleration is not small, the full system is tracked only with an input-to-state stability property.

Proof: When angular acceleration of quadrotor becomes low, by Prop. 1, with properly selected gains k_R, k_Ω, there exists $\bar{\varepsilon}$ such that when $\varepsilon < \bar{\varepsilon}$ and the quadrotors yaw angles can be tracked exponentially. By Prop. 2, based on the assumption of low angular acceleration of the quadrotor, all configuration errors e_x, e_v, e_q, e_ω converge exponentially. Thus it explains the almost exponential convergence of full state errors, by applying Tychonoff's theorem [1, Theorem 11.4].

If the angular acceleration of the quadrotor is not low, the load position and load attitude controllers in Prop. 2 have the input-to-state stability property. Therefore the full system is only input-to-state stable. ∎

V. Robust Analysis and Simulation

In order to validate the stability of our controller, we perform a numerical simulation in Matlab. Our goal is try to track a circular load trajectory with a given desired yaw angle. The desired load trajectory and yaw angle are taken

TABLE II

SYSTEM PARAMETERS FOR SIMULATION (UNITS IN SI)

	Value		Value
m_L	0.087	m_Q	0.5
J_Q	$diag[2.32, 2.32, 0.4] \times 10^{-3}$	L	1
r	$[0.05, 0.05, -0.05]$		

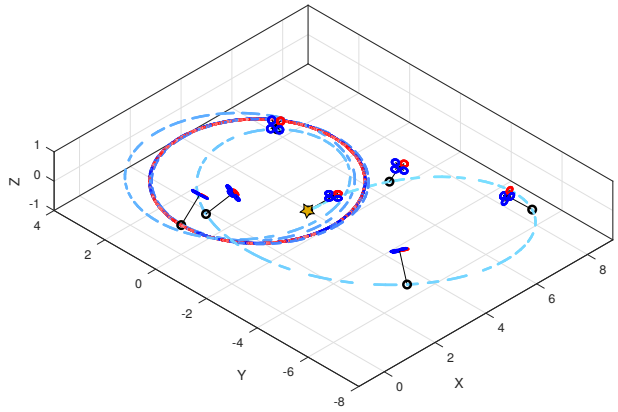

Fig. 3. Snapshots of the quadrotor along the executed motion (blue) as it tracks the desired load position (red). Notice the large initial errors in position, load and quadrotor attitude. This shows the convergences performance of the geometric controller $\mathscr{C}_O$ for the offset model. In these snapshots, our goal is track a desired circular load trajectory of a frequency $f = 0.3Hz$. We can observe the tiny final error when using offset geometric controller $\mathscr{C}_O$. A star-shaped marker is added to indicate the initial position of load. The load position tracking in the last 5 seconds are shown from the top view in Figure 4.

as,

$$x_L(t) = \begin{bmatrix} A_x \cdot [1 - cos(2\pi f t)] \\ A_y \cdot sin(2\pi f t) \\ A_z \end{bmatrix}, \tag{41}$$

$$\psi(t) = 0, \tag{42}$$

where $A_x = A_y = 3$ and $A_z = 0$. Other values of system parameters are shown in Table II.

We consider two controllers $\mathscr{C}_Z$ and $\mathscr{C}_O$ representing zero offset controller and offset controller, and apply them to our offset dynamical model. The controllers are simulated to track a desired circular payload trajectory. During the simulations, the frequency of circular movement f ranges from 0 to 0.3 and other parameters and initial conditions are kept in the same for two controllers, specifying the same large errors in the quadrotor attitude, the load attitude and the load position. Specifically, the initial load attitude is supposed as 90°, and there is also a large initial load position error. The desired time-varying load position trajectory and yaw angle are specified in (41), (42) and the system is simulated with the controller in Prop. 3. Figure 3 illustrates the convergence to the desired load position trajectory with our offset geometric controller $\mathscr{C}_O$, as well as snapshots of the quadrotor at fixed times. We also compare the final error of two controllers in Figure 4. The convergence performance of our offset geometric controller is better.

To compare the performances of the two controllers analytically, we also present the final error of load position by using two controllers to track the circular trajectory with different frequencies in Figure 5. For these two controllers,

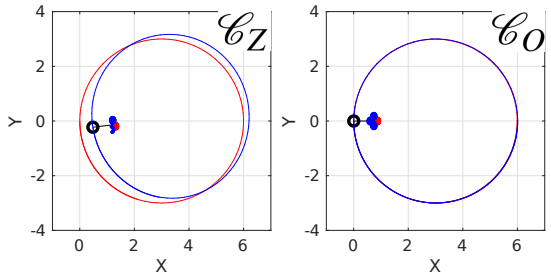

Fig. 4. Final load position tracking error for controller $\mathscr{C}_Z$ and $\mathscr{C}_O$ from top view. The simulations are launched when $f = 0.3Hz$ and the position error can be observed between the executed motion (blue) as it tracks the desired load position (red). We can see that controller $\mathscr{C}_O$ has much better convergence performance for load position tracking than controller $\mathscr{C}_Z$.

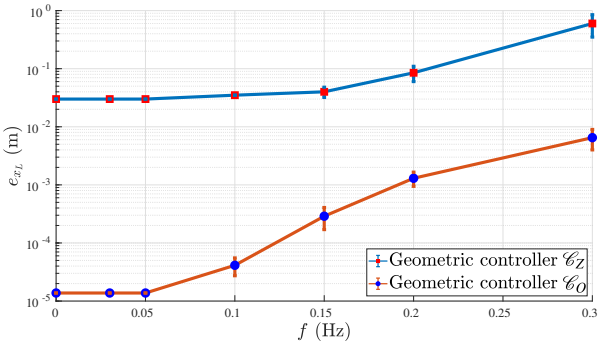

Fig. 5. Final load position error corresponding to several values of f by using controllers $\mathscr{C}_O$ and $\mathscr{C}_Z$. The error bar indicates the variance of final error for some cases if it oscillates. We can see that the controller $\mathscr{C}_O$ is far better than $\mathscr{C}_Z$ for any f. Notice that the final error of load position generated by the controller $\mathscr{C}_O$ is almost zero when f is small, while the controller $\mathscr{C}_Z$ always results in an apparent final error, even if the orbit frequency is small.

the final error increases in both cases, as the orbit frequency increases. The geometric controller $\mathscr{C}_O$ shows advantages on robustness and stability. On the one hand for aggressively moving scenario, the zero offset geometric controller $\mathscr{C}_Z$ has a final error of $0.6m$ when f is $0.3Hz$. However, our geometric control is more robust and better rejects the load position error, with the final error converging to only $0.0067m$, which is two orders of magnitude better. On the other hand, even for stationary case when $f = 0Hz$, the final error of load position by using controller $\mathscr{C}_Z$ doesn't converge to zero, while the one using $\mathscr{C}_O$ has no apparent final error. Thus our offset geometric controller is recommended to be used in case of quadrotor with suspended load for both high speed moving and hovering scenarios, if the offset from the quadrotor's center-of-mass to the suspension point cannot be ignored.

Remark 7: In the experiments, we can typically adjust the suspension point to the bottom base of the quadrotor so that the offset only exists in the z direction in the body-fixed frame. We rerun the simulation with the same initial conditions as above with the offset vector $r = [0m, 0m, -0.05m]$. We find that the final error of load position is 0.0001m when the frequency $f = 0.3Hz$ when using controller $\mathscr{C}_O$, whereas the error is 0.1m when using controller $\mathscr{C}_Z$. This result motivates us to implement this controller for future

experiments.

VI. Conclusion

We have presented a coordinate-free development of the dynamics of a quadrotor with a cable suspended load, where the suspension point is at an offset from the CoM. Based on an assumption of low angular acceleration of quadrotor, we have built the differential flatness of the system and have utilized it to design nominal trajectories. A nonlinear geometric control design is presented, that enables tracking of either the quadrotor attitude, the load attitude or the load position. The stability properties of the controllers are formally proved. With numerical simulations, we have demonstrated that our proposed geometric controller has much better performance for tracking desired payload trajectories than traditional geometric control where the offset is not considered,

Appendix

A. Derivation of the Dynamics for the Quadrotor with Load Suspended with an offset from the CoM of quadrotor to the suspension point

The geometric kinematic relation between quadrotor and load are given by

$$x_Q = x_L - Lq - Rr,$$
$$v_Q = v_L - L\dot{q} - R\hat{\Omega}r.$$

Thus, the Lagrangian of system can be written as

$$\begin{aligned}\mathscr{L} =& \frac{1}{2}m_Q||v_L - L\dot{q} - R\hat{\Omega}r||^2 + \frac{1}{2}\Omega^T J\Omega + \frac{1}{2}m_L||v_L||^2 \\ & - m_Q g e_3 \cdot (x_L - Lq - Rr) - m_L g e_3 \cdot x_L.\end{aligned}$$

When x_L has a variation δx_L,

$$\begin{aligned}\delta\mathscr{L}_{x_L} =& \delta\dot{x}_L \cdot ((m_Q + m_L)v_L - m_Q(R\hat{\Omega}r + L\dot{q})) \\ & - (m_Q + m_L)\delta x_L \cdot g e_3.\end{aligned} \tag{43}$$

When R has a variation δR,

$$\begin{aligned}\delta\mathscr{L}_R =& \delta\Omega(J\Omega - m_Q\hat{r}R^T(v_L - L\dot{q})) \\ & - \Omega \cdot m_Q\hat{r}(\delta R)^T(v_L - L\dot{q}) + m_Q\delta R r \cdot g e_3.\end{aligned}$$

Substituting (5) into the equation above, we have

$$\begin{aligned}\delta\mathscr{L}_R =& \dot{\eta}(J\Omega - m_Q r R^T(v_L - L\dot{q})) - \eta \cdot \hat{\Omega}J\Omega \\ & + \eta \cdot (m_Q r\hat{\Omega}R^T(v_L - L\dot{q}) + M_Q\hat{r}R^T g e_3).\end{aligned} \tag{44}$$

Similarly, we have

$$\begin{aligned}\delta\mathscr{L}_q =& \dot{\xi} \cdot (m_Q L^2\hat{q}\dot{q} - m_Q L\hat{q}(v_L - R\hat{\Omega}r)) \\ & + \xi \cdot m_Q L(\hat{q}g e_3 - \dot{\hat{q}}(v_L - R\hat{\Omega}r)).\end{aligned} \tag{45}$$

Then applying D'Alembert principle yields the following three equations of motion:

$$\begin{aligned}&\int_{t_0}^{t_1} \delta\dot{x}_L \cdot ((m_Q + m_L)v_L - m_Q(R\hat{\Omega}r + L\dot{q})) \\ &- (m_Q + m_L)\delta x_L \cdot g e_3 + \delta x_L \cdot f R e_3 dt = 0, \\ &\int_{t_0}^{t_1} \dot{\eta}(J\Omega - m_Q r R^T(v_L - L\dot{q})) - \eta \cdot \hat{\Omega}J\Omega + \eta \cdot (m_Q r\hat{\Omega}R^T \\ &(v_L - L\dot{q}) + m_Q\hat{r}R^T g e_3) + \eta \cdot (-\hat{r}R^T f R e_3 + M)dt = 0, \\ &\int_{t_0}^{t_1} \dot{\xi} \cdot (m_Q L^2\hat{q}\dot{q} - m_Q L\hat{q}(v_L - R\hat{\Omega}r)) + \xi \cdot m_Q L \\ &(\hat{q}g e_3 - \dot{\hat{q}}(v_L - R\hat{\Omega}r)) - \xi \cdot (L\hat{q}f R e_3)dt = 0.\end{aligned}$$

By integration by parts, the first equation can be simplified as:

$$(m_Q + m_L)(\ddot{x}_L + g e_3) = f R e_3 + m_Q L\ddot{q} + m_Q(R\hat{\Omega}^2 + R\dot{\hat{\Omega}})r, \tag{46}$$

similarly for the second one, we have

$$J\dot{\Omega} + \hat{\Omega}J\Omega = -m_Q L\hat{r}R^T(\ddot{q} + \frac{f}{m_Q L}R e_3) + m_Q\hat{r}R^T(\ddot{x}_L + g e_3) + M, \tag{47}$$

and for the third one, we also have

$$\hat{q}^2[L\ddot{q} + \frac{f}{m_Q}R e_3 - (g e_3 + \dot{v}_L - R\hat{\Omega}^2 r - R\dot{\hat{\Omega}}r)] = 0, \tag{48}$$

which indicates that

$$\dot{\omega} = \frac{1}{L}q \times [(\ddot{x}_L + g e_3 - R\hat{\Omega}^2 r - R\dot{\hat{\Omega}}r) - \frac{f}{m_Q}R e_3]. \tag{49}$$

Moreover, we have

$$\ddot{q} = \dot{\omega} \times q - (\dot{q} \cdot \dot{q})q. \tag{50}$$

Substituting (50) to (46), (47), we could have the following relationship:

$$\begin{aligned}(m_L + m_Q)(\ddot{x}_L + g e_3) =& -m_Q L(\dot{q} \cdot \dot{q})q + f R e_3 + m_Q(R\dot{\hat{\Omega}} + R\hat{\Omega}^2)r \\ & + m_Q\hat{q}^2[(R\hat{\Omega}^2 r + R\dot{\Omega}r) + \frac{f}{m}R e_3], \\ J\dot{\Omega} + \hat{\Omega}J\Omega =& -m_Q L\hat{r}R^T(q \cdot \frac{f}{m_Q L}R e_3 - (\dot{q} \cdot \dot{q}))q - m_Q\hat{r}R^T\hat{q}^2 \\ & (R\hat{\Omega}^2 r + R\dot{\hat{\Omega}}r) + m_Q\hat{r}R^T(\ddot{x}_L + g e_3) + M.\end{aligned}$$

Together with (49), the equations above can be simplified into a more compact form, as shown in (7), (8), (9), (10).

References

[1] H. K. Khalil, *Nonlinear Control*. New Jersey: Prentice Hall, 2002.

[2] P. Kotaru, G. Wu, and K. Sreenath., "Differential-flatness and control of multiple quadrotors with a payload suspended through flexible cables," in *Indian Control Conference (ICC)*, 2018, pp. 352–357.

[3] T. Lee, "Geometric control of multiple quadrotor uavs transporting a cable-suspended rigid body," in *IEEE Conference on Decision and Control*, 2014, pp. 6155–6160.

[4] T. Lee, K. Sreenath, and V. Kumar, "Geometric control of cooperating multiple quadrotor uavs with a suspended payload," in *IEEE Conference on Decision and Control*, 2013, pp. 5510–5515.

[5] D. Mellinger, Q. Lindsey, M. Shomin, and V. Kumar, "Design, modeling, estimation and control for aerial grasping and manipulation," in *IEEE/RSJ International Conference on Intelligent Robots and Systems*, 2011, p. 26682673.

[6] I. Palunko, R. Fierro, and P. Cruz, "Trajectory generation for swing-free maneuvers of a quadrotor with suspended payload: A dynamic programming approach," in *IEEE International Conference on Robotics and Automation*, 2012, pp. 2691–2697.

[7] J. A. Schultz and T. Murphey, "Trajectory generation for underactuated control of a suspended mass," in *2012 IEEE International Conference on Robotics and Automation*, 2012, pp. 123–129.

[8] K. Sreenath, T. Lee, and V. Kumar, "Geometric control and differential flatness of a quadrotor uav with a cable-suspended load," in *IEEE International Conference on Decision and Control*, 2013, pp. 2269-2274.

[9] K. Sreenath, N. Michael, and V. Kumar, "Trajectory generation and control of a quadrotor with a cable-suspended load - a differentially-flat hybrid system," in *IEEE International Conference on Robotics and Automation*, 2013, pp. 4873-4880.

[10] G. P. Starr, J. E. Wood, and R. Lumia, "Rapid transport of suspended payloads," *Proceedings of the 2005 IEEE International Conference on Robotics and Automation*, pp. 1394–1399, 2005.

[11] S. Tang and V. Kumar, "Mixed integer quadratic program trajectory generation for a quadrotor with a cable-suspended payload," in *IEEE International Conference on Robotics and Automation*, 2015, pp. 2216–2222.

[12] J. Thomas, G. Loianno, J. Polin, K. Sreenath, and V. Kumar, "Toward autonomous avian-inspired dynamic grasping and perching," *Bioinspiration & Biomimetics*, vol. 9, no. 2, pp. 025 010–025 024, Jun. 2014.

[13] G. Wu and K. Sreenath, "Geometric control of quadrotors transporting a rigid-body load," in *IEEE Conference on Decision and Control*, 2014, pp. 6141–6148.